Perspectives of advanced thermal management in solar thermochemical syngas production using a counter-flow solid-solid heat exchanger

Christoph Falter, Andreas Sizmann, and Robert Pitz-Paal

Citation: AIP Conference Proceedings **1850**, 100005 (2017); doi: 10.1063/1.4984462
View online: http://dx.doi.org/10.1063/1.4984462
View Table of Contents: http://aip.scitation.org/toc/apc/1850/1
Published by the American Institute of Physics

Perspectives of Advanced Thermal Management in Solar Thermochemical Syngas Production Using a Counter-Flow Solid-Solid Heat Exchanger

Christoph Falter[1,a)], Andreas Sizmann[1,b)] and Robert Pitz-Paal[2,c)]

[1]*Bauhaus Luftfahrt, Willy-Messerschmitt-Straße 1, 82024 Taufkirchen, Germany*
[2]*DLR, Institute of Solar Research, Linder Höhe, 51147 Köln, Germany*

[a)]Corresponding author: christoph.falter@bauhaus-luftfahrt.net
[b)]andreas.sizmann@bauhaus-luftfahrt.net
[c)]robert.pitz-paal@dlr.de

Abstract. A modular reactor model is presented for the description of solar thermochemical syngas production involving counter-flow heat exchangers that recuperate heat from the solid phase. The development of the model is described including heat diffusion within the reactive material as it travels through the heat exchanger, which was previously identified to be a possibly limiting factor in heat exchanger design. Heat transfer within the reactive medium is described by conduction and radiation, where the former is modeled with the three-resistor model and the latter with the Rosseland diffusion approximation. The applicability of the model is shown by the analysis of heat exchanger efficiency for different material thicknesses and porosities in a system with 8 chambers and oxidation and reduction temperatures of 1000 K and 1800 K, respectively. Heat exchanger efficiency is found to rise strongly for a reduction of material thickness, as the element mass is reduced and a larger part of the elements takes part in the heat exchange process. An increase of porosity enhances radiation heat exchange but deteriorates conduction. The overall heat exchange in the material is improved for high temperatures in the heat exchanger, as radiation dominates the energy transfer. The model is shown to be a valuable tool for the development and analysis of solar thermochemical reactor concepts involving heat exchange from the solid phase.

INTRODUCTION

The limited amount of fossil hydrocarbon fuels together with concerns about the greenhouse gas emissions have lead to increased efforts of research and development focused on sustainable alternative fuels. Among the different options, the solar thermochemical production pathway shows a promising potential in terms of solar-to-fuel energy conversion efficiency because it makes use of the whole spectrum of solar energy. A field of heliostats or dishes is used to concentrate sunlight onto a receiver carrying a reactive material which is heated to temperatures in the range of 1800 K. In the second step of the process, the material is cooled by several hundred Kelvin and contacted with CO_2 and/or H_2O. The gases are split into CO and/or H_2 and O_2, where the latter is incorporated into the lattice of the reactive material to return it to its initial state. The synthesis gas mixture of CO and H_2 can then be converted into hydrocarbon fuels in the Fischer-Tropsch process. Among the materials used for this process are iron oxide,[1] zinc oxide[2] and cerium oxide,[3] where the latter has shown a significant advancement of experimental energy conversion efficiency.[4–6]

Most of the process steps of the solar thermochemical pathway are already used on an industrial scale such as seawater desalination for the large-scale provision of H_2O,[7] the concentration of solar energy,[8] Fischer-Tropsch synthesis,[9] and gas storage and distribution. Solar thermochemical conversion of CO_2 and H_2O to syngas, on the other hand, is currently the focus of several research projects and has a decisive influence on the whole process: thermochemical energy conversion efficiency defines the size of the solar concentration facility and therefore

SolarPACES 2016
AIP Conf. Proc. 1850, 100005-1–100005-8; doi: 10.1063/1.4984462
Published by AIP Publishing. 978-0-7354-1522-5/$30.00

determines to a large degree the economics of the process as well as its ecological performance.[10] The two-step process requires the thermal cycling of the reactive material between the oxidation and reduction temperature and thus the input of significant amounts of energy.[11,12] This is true especially for nonstoichiometric reactions such as the ones with ceria remaining in its fluorite structure, where the amount of fuel produced per cycle and per unit mass of material is smaller than for stoichiometric reactions such as for the ZnO-cycle. To increase the efficiency of the cycle, it is therefore imperative to recuperate the energy used for thermal cycling with an advanced thermal management.[13] For the case of ceria, on the one hand, fundamental thermodynamic analyses exist that indicate the potential of the cycle.[11,13,14] On the other, several reactor concepts involving heat recuperation from the solid and gaseous phase have been proposed recently.[15–18] However, to analyze the wide parameter space of solar thermochemical reactors, a generic reactor model is required that can describe technically interesting concepts and that provides the means to analyze their realistic efficiency potentials. Such a generic reactor model incorporating counter-flow solid-solid heat exchange from the reactive material is described in,[12] where the assumption of infinitely fast heat diffusion in the reactive material was made. Here, the model is extended to include modeling of the heat diffusion process which enables the description of realistic heat exchanger concepts and thus provides guidance for the design of novel implementations of particle reactors.

GENERIC REACTOR MODEL WITH COUNTER-FLOW SOLID-SOLID HEAT EXCHANGE

The physical generic reactor concept for a two-step thermochemical process consists of a reduction chamber, an oxidation chamber, and (n-2) intermediate chambers for heat exchange (Fig. 1). The residence time in each of the reaction chambers can be chosen independently as multiples of the residence time in the heat exchanger chambers by allowing a larger number of elements per reaction chamber. In this way, requirements due to kinetics of the oxidation and reduction reactions can be met and the reactions run to completion. Assuming initial species concentrations and constant temperatures in the reaction chambers, the evolving nonstoichiometry and amount of syngas produced are calculated with mass conservation and equilibrium thermodynamics. The temperatures in the heat exchanger are then derived using a model which applies energy conservation between thermal energy stored in the elements of reactive material, internal heat exchange by radiation, and energy losses to the environment by convection and radiation. Without loss of generality of the approach, we assume ceria as the reactive medium. A vacuum pump establishes the reducing atmosphere.

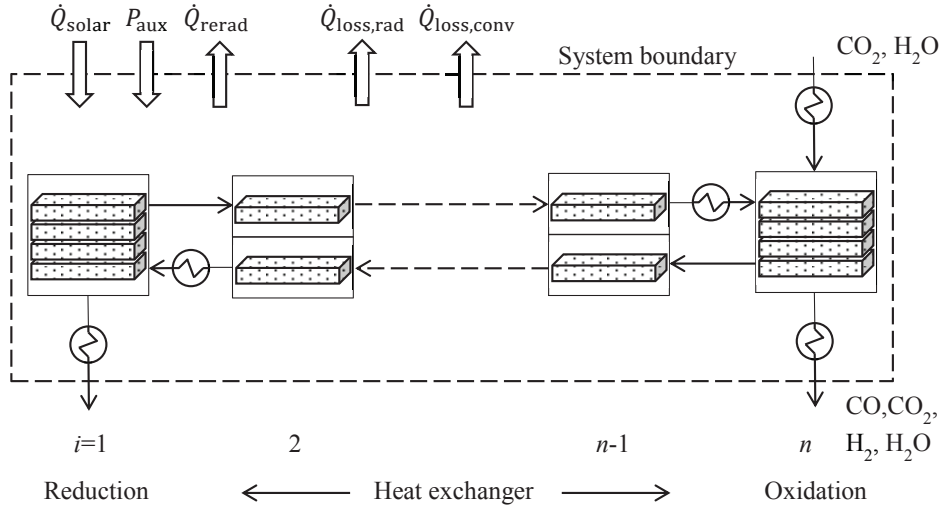

FIGURE 1. Schematic of generic rector model including n chambers, one for reduction (i=1) and oxidation (i=n), and n-2 physical heat exchanger chambers (i=2…n-1)

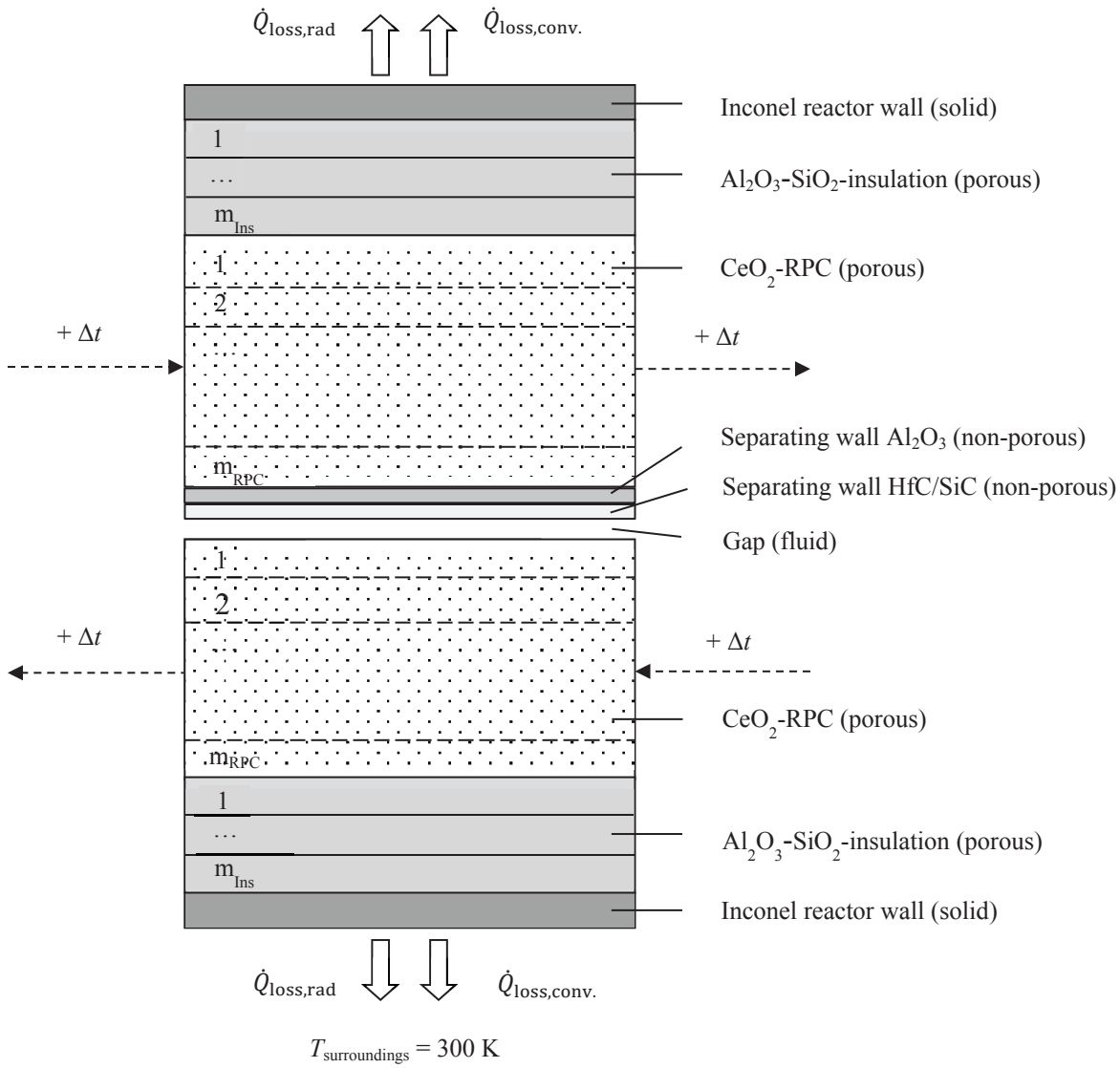

FIGURE 2. Schematic of one representative heat exchanger chamber for the modeling of radiation heat exchange between chamber halves and internal heat transfer in the reactive medium and adjacent insulation. Indicated are also the boundary conditions and the movement of the reactive material.

As part of an earlier study, the influence of the separating wall was neglected and heat diffusion within the elements of reactive material was assumed to proceed instantly.[12] In a baseline case with i = 80 chambers, a residence time of 10 s per chamber, and reduction and oxidation temperatures of 1800 K and 1000 K, respectively, a heat exchanger efficiency of close to 80% was found. Removing the assumption of infinite heat conductivity of the material, the same study found the heat exchanger efficiency to be dependent on the internal heat transfer processes in the material. Therefore, it is of high interest to further investigate the influence of heat diffusion and of basic parameters of the heat exchanger on efficiency.

In the present study, a further evolution of the model is discussed, where the separating wall between counter-flow chambers (composed of two layers of Al_2O_3 and SiC/HfC) is taken into account and heat diffusion within the reactive material is modeled. As reactive material, a reticulated porous ceramic (RPC) made of pure ceria with 80% porosity is assumed.[5] A representative schematic of the computational domain is shown in Fig. 2. The RPC is subdivided into a number of layers with constant temperature. A physical gas-tight separation between the elements in their reduced and oxidized state is thus required to prevent gas cross-over. This separation is implemented with a

separating wall in the proposed reactor model, where the separating wall is assumed to be made of a material with high emissivity and thermal conductivity in order to reduce its influence on the radiation heat exchange. The separating wall does not present a radiation shield in a classical sense because of the direct contact with the element in the upper chamber. Through its high thermal conductivity and low mass, the separating wall quickly assumes the temperature of the element in the upper chamber half and its high emissivity enables effective thermal radiation heat exchange with the element in the lower chamber half. SiC/HfC was identified to possess the desired material properties for the separating wall, however, due to possible chemical reactions of SiC and CeO_2 at elevated temperatures, a direct contact is prevented through the introduction of an additional layer of solid Al_2O_3 which is commonly used as insulation material in its porous form. The non-porous Al_2O_3 (99.5% purity, 0% porosity) has a higher thermal conductivity of 35 W m^{-1} K^{-1} [19] (porous alumina: ≈0.2 W m^{-1} K^{-1} [20]) and is thus more suitable as a separating layer. The reactive RPC material and the adjacent Al_2O_3-SiO_2 insulation are modeled as homogenous porous domains, in which energy is transferred by radiation and conduction. The separating wall between the chamber halves is modeled as a solid domain (composed of layers of Al_2O_3 and SiC/HfC, each of 1 mm thickness), while the gap is modeled as a fluid domain. The fluid in the gap is assumed to be oxygen. The reactor wall is made from Inconel 600 and has a thickness of 0.003 m. Due to the low temperature level behind the insulation, also conventional steel would be appropriate for the reactor wall, however, Inconel 600 is chosen here analogous to recent experiments.[4,6,21,22] A computational study was performed to analyze heat exchanger efficiency as a function of insulation thickness. The thickness is chosen to be 0.1 m after the study showed that a further increase in thickness leads to only very small improvements in efficiency.

Governing Equations of Heat Exchange

Porous Domains

In the porous domains of the RPC and the insulation, the energy balance is the following.

$$\rho c_p \frac{\partial T}{\partial t} = \nabla\left(\lambda \nabla T\right) - \nabla \vec{q}_{\text{rad}} \tag{1}$$

Heat is transferred by radiation and conduction, where convection is neglected due to the fact that the gas in the pores of the RPC and surrounding it is stagnant and does not have a large volume to establish a convective flow, as well as following the reasoning in a previous publication,[23] where the authors argue that the contribution of free convection to overall heat transfer in packed beds is considered to be negligible for most cases.

Heat transfer by thermal radiation has been derived with different models in the literature which vary in the level of accuracy and computational expense. Here, a model is required that is able to accurately describe the heat exchange processes at comparably low computational cost since the chosen method of pseudo-time stepping leads to a large number of computations. The Rosseland diffusion approximation was shown to have an adequate accuracy at low computational cost[24,25] and is therefore chosen here. Energy conservation is then written in the following form.

$$\rho c_p \frac{\partial T}{\partial t} = \nabla\left[\left(\lambda + \lambda_{\text{rad}}\right)\nabla T\right] \tag{2}$$

λ is the effective thermal conductivity of the RPC and λ_{rad} is the equivalent thermal conductivity describing thermal radiation. λ_{rad} is expressed by

$$\lambda_{\text{rad}} = \frac{16\sigma T^3}{\beta_{\text{R}}}, \tag{3}$$

where β_{R} is the Rosseland mean attenuation coefficient and σ is the Stefan-Boltzmann constant.[26] In the following, a distinction is made between the derivation of the effective thermal conductivity for the RPC and the porous insulation.

Reticulated Porous Ceramic (RPC)

For a gray medium, as assumed here, β_{R} is equal to the extinction coefficient β of the medium which is defined as a function of porosity [27]

$$\beta = \Psi_1 \cdot \frac{\sqrt{1-\varphi}}{d_{\text{mean}}}, \tag{4}$$

with the parameter Ψ_1=1.765, porosity φ and the mean pore diameter d_{mean} which is defined as[27]

$$d_{\text{mean}} = 2.20\times10^{-3} \cdot \varphi + 4.59\times10^{-4}\ \text{m}. \tag{5}$$

For the description of effective thermal conductivity of a porous medium, in a previous publication[27] different models are compared with data derived from direct pore level simulations which are based on tomography scans of a reticulated porous ceramic. The authors find that the extended three resistor model which expresses the fitting parameter *f* as a function of porosity is able to describe with great accuracy the effective thermal conductivity of the sample. The effective thermal conductivity λ is then expressed as follows.

$$\lambda = (1-f)\frac{k_f}{\varphi + (1-\varphi)\frac{k_f}{k_s}} + f\left(\varphi k_f + (1-\varphi)k_s\right), \tag{6}$$

where f is the fitting parameter described by $f = \sqrt{g_0 - g_1 \cdot \varphi}$, g_0 and g_1 are 0.754 and 0.829[27], k_f and k_s are the thermal conductivities of the fluid and solid material, and φ is the porosity of the porous domain.

Insulation

The porous insulation is comprised of fibers of Al_2O_3 and SiO_2. As the pore mean diameter is not known, experimental values for the Rosseland mean attenuation coefficient and for the thermal conductivity are used to describe the thermal energy transfer across the insulation. The former are taken from Zhang et al.[28] and the latter from the manufacturer of the type M-35 buster insulation[20] which has also been used in experiments.[6,21,22,29]

Solid and fluid domains: in the solid and fluid domains, the law after Fourier is used to describe heat transfer by conduction.

Heat exchange between chamber halves: heat exchange between the chamber halves, i.e. between the lower side of the separating wall and the RPC in the lower chamber half is modeled assuming heat exchange between infinite flat plates and heat conduction through the fluid phase (assumed to be oxygen).

Heat loss to the surroundings: heat is lost through radiation and convection from the reactor wall to the surroundings which are assumed to be at 300 K.

The numerical solution is derived by solving the system of non-linear equations in MATLAB by choosing a starting point for the temperatures and using the method of pseudo-continuous time stepping to approximate the steady-state of the system.

Material Properties

The convective heat transfer coefficient from the reactor wall to the surroundings at 300 K is 15 W m^{-1} K^{-1}.[30] The emissivity, thermal conductivity, specific heat capacity, and density of the reactor wall made from Inconel 600 are taken from [31]. Its thickness is chosen to be 3 mm. The emissivity of the Al_2O_3-SiO_2 insulation is from [32], its radiative extinction coefficient from [28], its thermal conductivity and density from [20], and its specific heat capacity from [33]. Effective radiative properties and parameters for the modeling of combined conduction and radiation in the solid and fluid domains are taken from direct numerical pore-level simulations for the RPC material[27] and from [27,28] for the porous insulation. The emissivity of the CeO_2-RPC is used from [32] and the properties for the three resistor model to calculate the effective thermal conductivity from [27]. The thermal conductivity of solid CeO_2 is taken from [34], its density from [35], and its specific heat capacity from [36]. The thermal conductivity of oxygen and the specific heat capacity of oxygen, carbon monoxide, and carbon dioxide from [37].

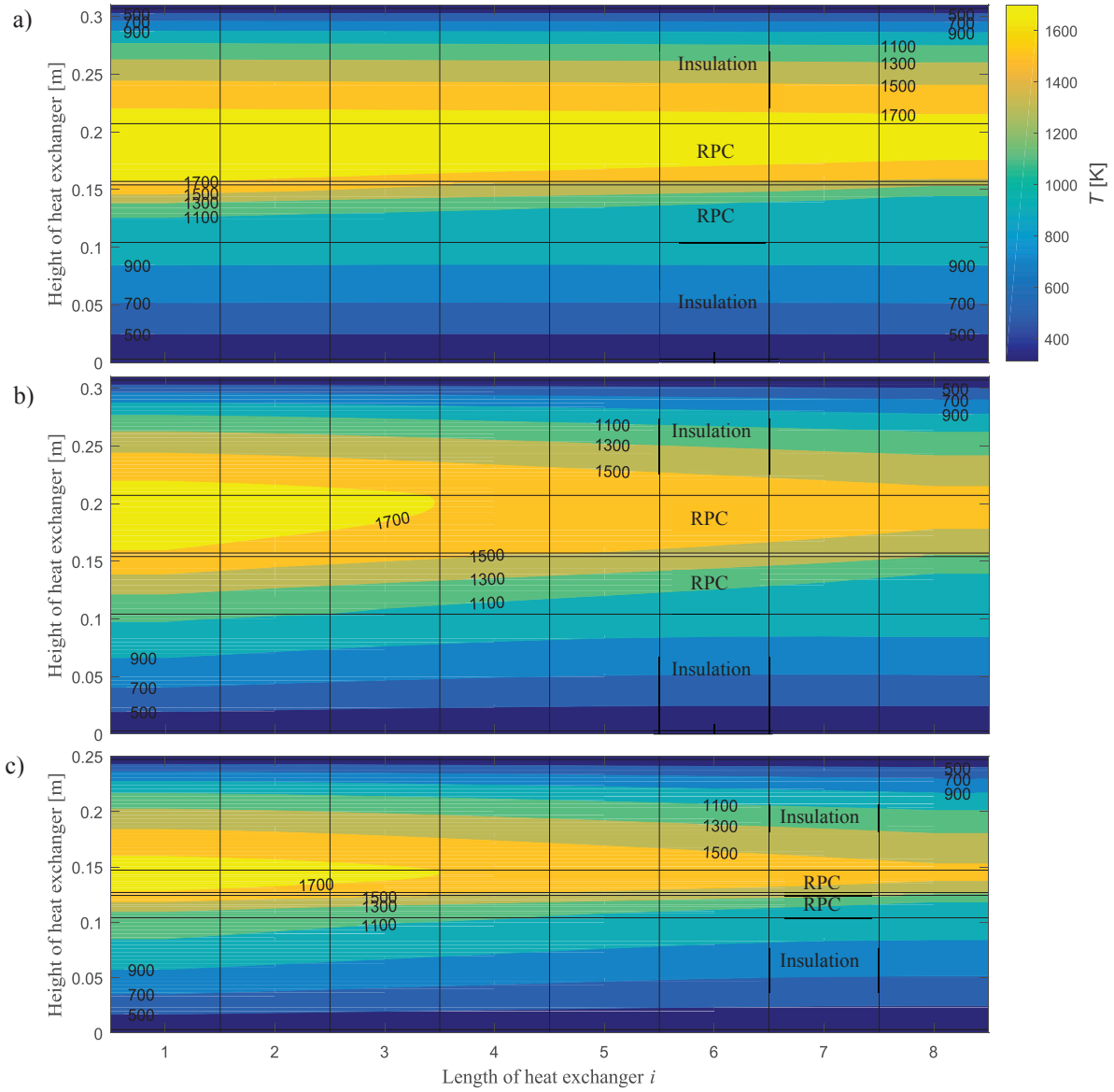

FIGURE 3. Temperature distribution in heat exchanger for three different configurations:
a) Porosity 40%, Thickness 0.05 m, b) Porosity 80%, Thickness 0.05 m, c) Porosity 40%, Thickness 0.02 m.

RESULTS

In the following, the influence of thickness and porosity of the reactive material on the efficiency of the heat exchanger is shown (Figure 3). Heat exchanger efficiency increases strongly with decreasing material thickness from η_{he}=0.188 at L=0.05 m to η_{he}=0.440 at L=0.02 m (compare a) with c) in Fig. 3). This significant improvement is due to the fact that for a given heat exchanger length and residence time of the elements, there is a finite time for the thermal energy to diffuse in the material. Thinner elements have a smaller mass and are heated more rapidly with a smaller temperature difference over the material. For larger thicknesses, parts of the material are participating poorly or not at all in the heat exchange between hot and cold elements, decreasing heat exchanger efficiency, as can be clearly seen in the lower chamber halves of the RPC with thickness 0.05 m as compared to the thinner elements.

The heat exchanger efficiency also increases strongly with porosity from η_{he}=0.188 at φ=0.4 to η_{he}=0.416 at φ=0.8 (compare a) to b) in Fig.3). Equally to a reduction of element thickness, an increase in porosity reduces the element mass and has thus a positive influence on heat exchanger efficiency. Furthermore, the effect of porosity on overall heat transfer is based on a trade-off between improved radiation heat exchange and deteriorated thermal conductivity of the material: on the one hand, by increasing the porosity, the extinction coefficient is decreased in Eq. 4, leading to a higher equivalent thermal conductivity in Eq. 3. On the other hand, a higher porosity decreases the amount of solid material and thus the effective thermal conductivity. The overall effect on the thermal conductivity including radiation and conduction thus depends on which mode of heat transfer is dominating. At high temperatures above about 1000 K, radiation heat exchange dominates the thermal energy transfer within the material. Due to a reduced mass and enhanced thermal conductivity, an improvement of heat exchange between the hot and cold elements is seen with increasing porosity at the given temperatures.

Summary

A generic reactor model that can be used for the description of a large number of different reactor concepts is enhanced to include the description of internal heat diffusion within the reactive material. The model describes heat transfer by radiation and conduction, where the former is expressed with the Rosseland diffusion approximation and the latter with the three resistor model, while convection is neglected. This extension allows the model to include the effect of heat diffusion which has been identified to be a crucial design parameter for heat exchangers working with solid-solid heat recuperation. The model development including assumptions and material parameters is documented and its applicability is demonstrated in the analysis of heat exchanger efficiency as a function of material thickness and porosity. For a chosen operating point with oxidation and reduction temperatures of 1000 K and 1800 K, and 8 heat exchanger chambers, heat exchanger efficiency was shown to increase significantly from 18.8% to 44.0% for a reduction of material thickness from 0.05 m to 0.02 m, and to 41.6% for an increase of porosity from 40% to 80%. The model is therefore capable of describing crucial design parameters of heat exchanger concepts for solar thermochemical syngas production.

ACKNOWLEDGMENTS

This project has received funding from the European Union's Horizon 2020 research and innovation programme under grant agreement No 654408 (SUN-to-LIQUID). This document reflects the authors' view only and the INEA must not be taken as responsible for any use that may be made of the information it contains.

REFERENCES

1. Nakamura, T. Hydrogen production from water utilizing solar heat at high temperatures. *Sol. Energy* **19,** 467–475 (1977).
2. Palumbo, R. *et al.* The production of Zn from ZnO in a high-temperature solar decomposition quench process—I. The scientific framework for the process. *Chem. Eng. Sci.* **53,** 2503–2517 (1998).
3. Abanades, S. & Flamant, G. Thermochemical hydrogen production from a two-step solar-driven water-splitting cycle based on cerium oxides. *Sol. Energy* **80,** 1611–1623 (2006).
4. Chueh, W. C. *et al.* High-flux solar-driven thermochemical dissociation of CO_2 and H_2O using nonstoichiometric ceria. *Science* **330,** 1797–1801 (2010).
5. Furler, P. *et al.* Solar thermochemical CO_2 splitting utilizing a reticulated porous ceria redox system. *Energy and Fuels* **26,** 7051–7059 (2012).
6. Marxer, D. A. *et al.* Demonstration of the entire production chain to renewable kerosene via solar-thermochemical splitting of H_2O and CO_2. *Energy & Fuels* **29,** 3241–3250 (2015).
7. Fritzmann, C., Lowenberg, J., Wintgens, T. & Melin, T. State-of-the-art of reverse osmosis desalination. *Desalination* **216,** 1–76 (2007).
8. National Renewable Energy Laboratory. Concentrating solar power projects. (2011). at <http://www.nrel.gov/csp/solarpaces/power_tower.cfm>
9. Overtoom, R., Fabricius, N. & Leenhouts, W. Shell GTL , from Bench scale to World scale. *Proc. 1st Annu. Gas Process. Symp. 10–12 January 2009, Doha, Qatar* 378–386 (2009). doi:10.1016/B978-0-444-53292-3.50046-8

10. Falter, C., Batteiger, V. & Sizmann, A. Climate Impact and Economic Feasibility of Solar Thermochemical Jet Fuel Production. *Environ. Sci. Technol.* **50,** 470–477 (2016).
11. Chueh, W. C. & Haile, S. M. A thermochemical study of ceria: exploiting an old material for new modes of energy conversion and CO_2 mitigation. *Philos. Trans. A. Math. Phys. Eng. Sci.* **368,** 3269–3294 (2010).
12. Falter, C. P., Sizmann, A. & Pitz-Paal, R. Modular reactor model for the solar thermochemical production of syngas incorporating counter-flow solid heat exchange. *Sol. Energy* **122,** 1296–1308 (2015).
13. Lapp, J., Davidson, J. H. & Lipiński, W. Efficiency of two-step solar thermochemical non-stoichiometric redox cycles withheat recovery. *Energy* **37,** 591–600 (2012).
14. Krenzke, P. T. & Davidson, J. H. On the Efficiency of Solar H_2 and CO Production via the Thermochemical Cerium Oxide Redox Cycle: The Option of Inert-Swept Reduction. *Energy & Fuels* 150206073859007 (2015). doi:10.1021/ef502601f
15. Diver, R. B., Miller, J. E., Allendorf, M. D., Siegel, N. P. & Hogan, R. E. Solar Thermochemical Water-Splitting Ferrite-Cycle Heat Engines. *J. Sol. Energy Eng.* **130,** 041001 (2008).
16. Lapp, J., Davidson, J. H. & Lipiński, W. Heat Transfer Analysis of a Solid-Solid Heat Recuperation System for Solar-Driven Nonstoichiometric Cycles. *J. Sol. Energy Eng.* **135,** 031004 (2013).
17. Chandran, R. B., De Smith, R. M. & Davidson, J. H. Model of an integrated solar thermochemical reactor/reticulated ceramic foam heat exchanger for gas-phase heat recovery. *Int. J. Heat Mass Transf.* **81,** 404–414 (2015).
18. Ermanoski, I., Siegel, N. P. & Stechel, E. B. A New Reactor Concept for Efficient Solar-Thermochemical Fuel Production. *J. Sol. Energy Eng.* **135,** 031002 (2013).
19. Accuratus. Aluminum Oxide, Al2O3 Ceramic Properties. (2016). at <http://accuratus.com/alumox.html>
20. Zircar Zirconia. Fibrous Insulation - Type Buster M35. (2015). at <http://www.zircarzirconia.com/product-literature/buster.php>
21. Furler, P., Scheffe, J. R. & Steinfeld, A. Syngas production by simultaneous splitting of H_2O and CO_2 via ceria redox reactions in a high-temperature solar reactor. *Energy Environ. Sci.* **5,** 6098 (2012).
22. Furler, P. *et al.* Thermochemical CO_2 splitting via redox cycling of ceria reticulated foam structures with dual-scale porosities. *Phys. Chem. Chem. Phys.* **16,** 10503–11 (2014).
23. Tsotsas, E. & Martin, H. Thermal conductivity of packed beds: A review. *Chem. Eng. Process. Process Intensif.* **22,** 19–37 (1987).
24. Petrov, V. A. Combined radiation and conduction heat transfer in high temperature fiber thermal insulation. *Int. J. Heat Mass Transf.* **40,** 2241–2247 (1997).
25. Wang, F., Shuai, Y., Tan, H. & Yu, C. Thermal performance analysis of porous media receiver with concentrated solar irradiation. *Int. J. Heat Mass Transf.* **62,** 247–254 (2013).
26. Howell, J. R., Siegel, R., Mengüc, M. & Pinar, R. *Thermal Radiation Heat Transfer*. (CRC Press, 2011).
27. Suter, S., Steinfeld, A. & Haussener, S. Pore-level engineering of macroporous media for increased performance of solar-driven thermochemical fuel processing. *Int. J. Heat Mass Transf.* **78,** 688–698 (2014).
28. Zhang, B., Zhao, S., He, X. & Du, S. High Temperature Thermal Physical Properties of High-alumina Fibrous Insulation. *J. Mater. Sci. Technol.* **23,** 860–864 (2007).
29. Chueh, W. C. & Haile, S. M. A thermochemical study of ceria: exploiting an old material for new modes of energy conversion and CO_2 mitigation. *Philos Trans. A Math Phys Eng Sci* **368,** 3269–3294 (2010).
30. Hischier, I., Hess, D., Lipiński, W., Modest, M. & Steinfeld, A. Heat Transfer Analysis of a Novel Pressurized Air Receiver for Concentrated Solar Power via Combined Cycles. *J. Therm. Sci. Eng. Appl.* **1,** 041002 (2009).
31. Special Metals. Inconel Alloy 600. (2015). at <www.specialmetals.com/documents/Inconel alloy 600.pdf>
32. Touloukian, Y. S. & DeWitt, D. P. *Thermophysical Properties of Matter - The TPRC Data Series--Vol.8 Thermal Radiative Properties - Nonmetallic Solids*. (CINDAS/Purdue University, 1972).
33. Furler, P. Solar thermochemical CO_2 and H_2O splitting via ceria redox reactions. (Dissertation, ETH Zürich, 2014). doi:http://dx.doi.org/10.3929/ethz-a-010207593
34. Touloukian, Y. S., Powell, R. W., Ho, C. Y. & Klemens, P. G. *Thermophysical Properties of Matter - The TPRC Data Series--Vol.2. Thermal Conductivity - Nonmetallic Solids*. (CINDAS/Purdue University, 1971).
35. U.S. Environmental Protection Agency. *Toxicological Review Cerium Oxide and Cerium Compounds*. (2009).
36. Riess, I., Ricken, M. & Noelting, J. Specific heat of non-stoichiometric ceria (CeO_y). *Solid State Ionics* **18-19,** 725–726 (1986).
37. Kleiber, M. & Joh, R. *VDI-Wärmeatlas, Kapitel D*. (2013). doi:10.1007/978-3-642-19981-3